Journal of Applied Polymer Science

Thermomechanical and Water-Responsive Shape Memory Properties of Carbon Nanotubes-Reinforced Hyperbranched Polyurethane Composites

Sravendra Rana,[1] Jae Whan Cho,[1] Jong-Shin Park[2]
[1]Department of Textile Engineering, Konkuk University, Seoul 143-701, Korea
[2]Department of Biosystems & Biomaterials Science and Engineering, Seoul National University, Seoul 151-742, Korea
Correspondence to: J. W. Cho (E-mail: jwcho@konkuk.ac.kr)

ABSTRACT: Shape memory composites of hyperbranched polyurethane (HBPU) and acid-treated multi-walled carbon nanotubes (MWNTs) were prepared using an *in situ* polymerization method. HBPUs with different hard segments contents were synthesized via the $A_2 + B_3$ approach using poly(ethylene glycol) (PEG) as a soft segment, 4,4′-methylene bis(phenylisocynate), castor oil, and 1,4-butanediol as hard segment. Compared to HBPU, the HBPU/MWNT composites showed faster shape recovery and double the shape recovery stress in the thermomechanical shape memory test, which was dependent on the MWNTs content and HBPU hard segment content. The water-responsive shape memory effect of HBPU/MWNT composites was considered to result from the combined contribution of hydrophilic PEG and well dispersed MWNTs in highly branched HBPU molecules. © 2012 Wiley Periodicals, Inc. J. Appl. Polym. Sci. 000: 000–000, 2012

KEYWORDS: hyperbranched; composites; polyurethanes; shape memory; carbon nanotubes

Received 3 March 2011; accepted 22 February 2012; published online
DOI: 10.1002/app.37537

INTRODUCTION

Stimuli-responsive materials have attracted considerable interest owing to their response effects to external stimuli, such as temperature, light, electric field, pH, and water.[1–3] Compared to shape memory alloys, shape memory polymers have many advantages, such as an adjustable transition temperature, high shape stability, easy shaping, low cost, and good processing ability.[4–6] These materials have a broad range of applications in textiles, coating materials, elastomeric materials, actuators, and biomedical applications. Polyurethane (PU) block copolymer is the most studied shape memory polymer, which has a microphase separated heterogeneous structure of hard and soft segments. The hard segments phase with a high melting temperature acts as a physical crosslinker, whereas the soft segments phase serves as a molecular switch and facilitates the fixation of the temporary shape.[5,7,8] To improve the performance of PU, researchers have improved its thermal, electrical, and shape memory properties by adding nano-fillers to the polymeric matrix.[9,10]

Carbon nanotubes (CNTs) are considered an ideal reinforcing filler for high performance polymeric composites due to their excellent mechanical, thermal, and electrical properties.[11–13] The physico-chemical properties of polymer/CNTs composites are much better than conventional composites.[14] However, the aggregation of CNTs is still a drawback for their commercialization, which arises due to their strong intertube van der Waals interaction.[15] Several methods have been used to overcome this problem including mechanical mixing, solution mixing and *in situ* polymerization,[16–18] and covalent and noncovalent functionalization. Recently, hyperbranched polymers have been used effectively to enhance the dispersion of CNTs in polymer matrices owing to their highly functionalized three-dimensional globular nonentangled structure.[19,20] Hyperbranched polymers exhibit higher solubility, lower melt, and solution viscosity than linear counterparts.[21,22] In the viewpoint of shape memory materials, CNTs can be a very effective filler for enhancing high speed shape recovery and shape recovery force because the CNTs have a high thermal conductivity coefficient as well as excellent mechanical properties.

This study examined the combined effects of highly branched polymer structure and well dispersed CNTs on the thermomechanical and water-responsive shape memory properties by

Table I. Compounding Formulations of Samples Used in This Study

Sample codes	Feed weight (g)				MWNT-COOH (wt %)	HS content (wt %)	Mol weight (g/mol)	PDI (M_w/M_n)
	MDI	PEG	BD	Castor oil				
HBPU-36	2	6	0.27	1.1	-	36	9.6×10^4	2.1
HPU-NT-30	2	8	0.27	1.1	2	30	8.1×10^4	1.8
HPU-NT-36	2	6	0.27	1.1	2	36	-	-
HPU-NT-40	2	5	0.27	1.1	2	40	11.3×10^4	2.3
LPU-NT-36	2	4	0.27	-	2	36	6.7×10^4	1.5

preparing multi-walled carbon nanotubes (MWNTs) composites with hyperbranched polyurethane (HBPU). The shape memory properties of HBPU/MWNT composites including shape recovery stress analysis were also compared with those of linear PU-based MWNT composites.

EXPERIMENTAL

Materials

Poly(ethylene glycol) (PEG) with a molecular weight of 4000 g/mol was supplied by Kanto Chemical, Tokyo, and 1,4-butanediol (BD) was obtained from Junsei Chemical, Japan. 4,4′-Methylene bis(phenylisocynate) (MDI) and castor oil were purchased from Aldrich (St. Louis, MO). MWNTs with a diameter and length of approximately 10–20 nm and 20 μm, respectively, were acquired from Iljin Nanotech, Korea. Prior to use, the MWNTs were treated in a mixture of concentrated H_2SO_4/HNO_3 (3 : 1 v/v) at 100°C for 90 min, washed several times with distilled water, and dried under vacuum at 80°C for 2 days. Dimethylformamide (DMF) was used after purification using the conventional technique and stored with 4-Å type molecular sieves.

In Situ Polymerization of HBPU/MWNT Composites

HBPU was synthesized via the $A_2 + B_3$ approach using castor oil[23] as a multifunctional group, PEG as a soft segment, and MDI as a hard segment.[24] The pre-polymer was first prepared by a reaction of PEG with an excess of MDI at 70°C for 3 h without a catalyst. The isocyanate terminated pre-polymer and the unreacted diisocyanate were used as a A_2 monomer for the synthesis of the hyperbranched polymer. The addition of B_3 monomer, triglyceride of recinoleic acids (castor oil), and BD was then performed at 0°C with slow addition of dilute solution in DMF. An ultrasonic homogenized DMF solution of MWNTs was also added at the same temperature and then heated at 110°C for 2.5 h. After the reaction was complete, the final product solution was poured onto a glass Petri-dish, and the solvent was evaporated at 60°C in an oven followed by drying under vacuum to obtain the polymer films. Table I lists the composition of the HBPUs composites with different hard segments. To measure the effect of HBPU on the CNTs dispersion and other composite properties, a 36 wt % hard segment containing linear polyurethane-MWNT composites (LPU-NT-36) were also prepared using the same experimental conditions.

Measurements

The Fourier-transform infrared (FTIR, Jasco FT-IR 300E, Tokyo, Japan) spectra were recorded using an attenuated total reflectance method. The spectra were scanned at a resolution of 4 cm^{-1} and 40 scans for each measurement. The molecular weights of the hyperbranched polymers were determined by gel-permeation chromatography analysis (model 515, Water, Texas) with DMSO as the solvent at 1 mL/min flow rate and 50 μL injection volume. Differential scanning calorimetric (DSC, TA instrument 2010, New Castle, DE) measurements were carried out in the temperature range of −50°C to 250°C at a heating rate of 10 °C/min under nitrogen. The crystallinity of PEG soft segments in PU was determined by measuring the heat of crystallization upon cooling and using an enthalpy value of 197 J/g for 100% crystalline PEG.[25] Thermogravimetric analysis (TGA) was carried out in a TA Q50 system (New Castle, DE). The samples were scanned up to 800°C at a heating rate of 10 °C/min in the presence of nitrogen. The MWNT dispersion in the composites was analyzed from the surface morphology by transmission electron microscopy (TEM, JEM 2100F, JEOL, Tokyo, Japan), and scanning electron microscope (SEM, JSM-6380, JEOL, Tokyo, Japan). The SEM images were obtained from cross-sections of the fractured samples in liquid nitrogen and measured at an accelerating voltage of 20 keV. The samples for TEM analysis were prepared by ultracryomicrotomy with a Leica ultracut UCT at −60°C. The cryosections were collected individually in a sucrose solution and directly supported on a copper grid.

The mechanical properties of the samples were measured at room temperature using a tensile tester machine (Instron 4468) and dumb-bell shape sample. The dimensions of the test specimens were 60 × 2.9 × 0.4 mm^3. To quantify the shape fixity and shape recovery of the composites, the thermo-mechanical cyclic tensile test was conducted using a tensile tester (UTM, Lloyd LR 50 K, London, UK) in a temperature controlled chamber.[26] The specimen was stretched to a 100% elongation ratio at 60°C, above the switching transition temperature with a constant drawing speed of 10 mm/min and kept for 5 min at the same condition. The specimen was then cooled to −25°C and the temperature was maintained for 15 min to fix the temporary elongation. After removal of the load, the deformed length was then measured. The upper clamp was returned to the original position and the specimen was shrunk from ε_m (strain at 100% elongation) to ε_u (retention strain) due to the instant elastic recovery. Finally, the specimen was heated to 60°C to allow shape recovery with the resulting elongation returned to ε_p (recovery strain). The shape retention and shape recovery were calculated for three cycles using the following equations:

$$\text{Shaperetention}(\%) = (\varepsilon_u/\varepsilon_m) \times 100 \quad (1)$$

$$\text{Shaperecovery}(\%) = [(\varepsilon_m - \varepsilon_p)/\varepsilon_m] \times 100 \quad (2)$$

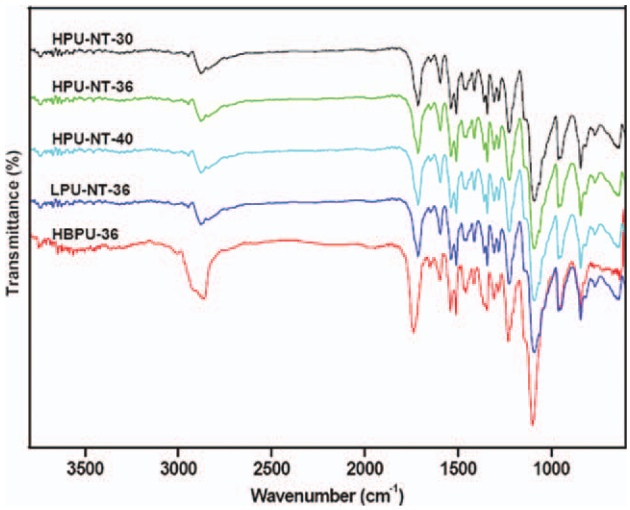

Figure 1. FTIR spectra of pure HBPU and its composites synthesized in this study. [Color figure can be viewed in the online issue, which is available at wileyonlinelibrary.com.]

RESULTS AND DISCUSSION

An *in situ* polymerization method was used to prepare the HBPU/MWNT composites, which enhanced the uniform dispersion of MWNTs in the polymer matrix. The synthesis of HBPU and its MWNT composites was confirmed by FTIR spectroscopy (Figure 1). The absorption band due to the —NCO group disappeared at 2250–2270 cm^{-1}, which confirms the completion of the reaction between —NCO and —OH groups for all the compositions. The absorption peaks at 1100–1250 cm^{-1} indicate the presence of —C—O—C in urethane, whereas the peaks at 2930 and 2860 cm^{-1} correspond to aliphatic —C—H stretching. The IR peaks at 1500–1575 cm^{-1} and 1600–1650 cm^{-1} were assigned to the —N—H and C=C stretching vibrations, respectively. The synthesis of HBPU was further confirmed by ^{1}H-NMR analysis.[24] ^{1}H-NMR analysis indicated peaks at δ 1.46–1.35 (CH_2 adjacent to urethane), δ 1.9 (CH_2 attached to C=C on the aliphatic side), δ 2.1–2.3 (CH_2 attached to C=C on the —O—C(=O) NH side), δ 7.10–7.35 (aromatic), δ 1.22–1.86 (CH_2 chain), δ 3.42–3.47 (CH_2 MDI), δ 8.3–8.5 (—N—H, urethane), and δ 0.84–0.89 (CH_3 terminal aliphatic), respectively. The ^{1}H-NMR data support not only the synthesis of HBPU but also the dendritic structure of the synthesized PU by calculating the degree of branching (DB), which was determined using the Frechet equation[27]: $DB = (D + T)/(D + T + L)$, where D, T, and L refer to the number of dendritic, terminal, and linear units in the polymer structure, respectively. DB was determined by a comparison of the reacted and unreacted B functional groups (hydroxyl group), and the same were compared with the model compounds. ^{1}H-NMR showed that the urethane (—O—CO—NH—) linkages derived from the —OH group of the B_3 monomers are sensitive to the number of B functional groups, which can be used to assign DB. The relative amounts of the aforementioned units were calculated by integrating the ^{1}H-NMR peaks of secondary C—H groups of substituted OH to urethane and unsubstituted OH. The DB value of the polymer was found to be 0.65–0.80.[24] For measuring the molecular weight (M_w) of synthesized PUs, PUs containing different hard segment contents were synthesized without addition of MWNTs. The M_w and polydispersity index (PDI) of the polymers (Table I) indicate that all the samples have good processing characteristics. The dispersion of CNTs within the polymer matrix is important for enhancing the shape memory composites, as with many other CNT composites. The superiority of

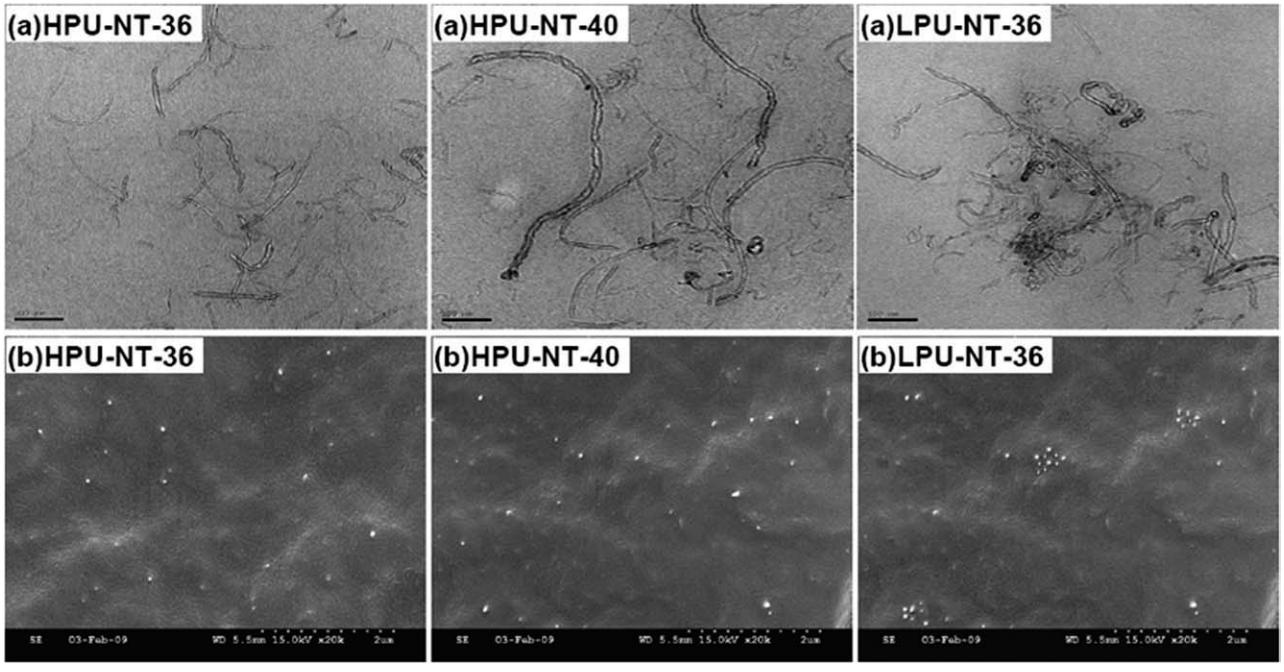

Figure 2. TEM (a) and SEM (b) images of the MWNT composites.

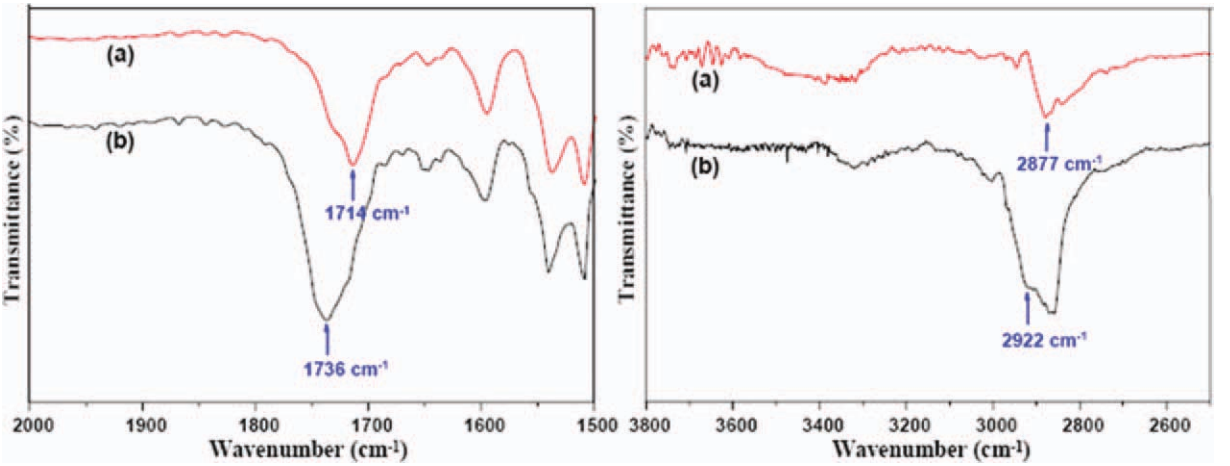

Figure 3. FTIR spectra for (a) HPU-NT-36 and (b) HBPU-36. [Color figure can be viewed in the online issue, which is available at wileyonlinelibrary.com.]

this hyperbranched polymer over the linear polymer for CNT dispersion was demonstrated. The dispersion of MWNTs was observed by TEM, as shown in Figure 2(a), where the individual dispersed MWNTs were observed in the HBPU matrix, by contrast, aggregated MWNTs were observed in the case of linear PU due to the poor dispersion of nanotubes. The debundling in HPU-NT-36 and HPU-NT-40 is due to the effect of the hyperbranched structure on the MWNTs dispersion. The dispersion of MWNTs was supported further by the SEM. Figure 2(b) shows SEM images of a cross-sectional fractured surface of the composites, where the bright dots indicate the broken ends of MWNTs. SEM and TEM images revealed the MWNTs to have a better dispersion in HBPU matrix compared to its linear counterpart.

The effect of the hyperbranched structure on the interaction between MWNT-COOH and HBPU was examined further using the FTIR spectra (Figure 3). The characteristic peaks at approximately 1735 cm^{-1} were assigned to the stretching vibration of the carbonyl peak (—C═O group) in HBPU. The carbonyl peak was shifted to 1714 cm^{-1} in the composites due to a molecular interaction between the MWNTs and PU. The CH_2 peak at 2923 cm^{-1} was also shifted to 2876 cm^{-1} in the case of the composites due to a hydrophobic interaction between the MWNT and long aliphatic chain present in the hyperbranched polymer.[28] The molecular interaction was supported further by N—H stretching. HBPU shows stretching at 3321–3315 cm^{-1} for N—H absorption, whereas the peak becomes broad in the composites due to the increase in hydrogen bonding N—H···O═C.

The thermal stability of the composite materials was examined by TGA. In Figure 4, all samples showed thermal degradation curves divided into two stages, corresponding to the soft and hard segment decomposition in PU.[24,29] TGA showed that the addition of MWNTs enhanced slightly the thermal stability of the composites. The thermal stability of HBPU composites was better than that of the linear PU composites. This might be due to the stronger interaction between the —COOH group of the MWNT and multifunctional groups of HBPU. The heat of crystallization (ΔH_c), heat of fusion (ΔH_f), crystallization temperature (T_c), melting temperature (T_m), and crystallinity percentage of the PEG crystals in the composites were measured and the results are summarized in Table II. Figure 5 shows the DSC curves of the samples, where the crystallinity and melting temperature of the composite materials depend on two important factors, the presence of MWNTs as well as the hard segment content. The crystallinity percentage decreased with increasing hard segment percentage due to decreased PEG content (Table II). The presence of little amount of MWNTs is useful to increase the crytallinity of the composite materials, as discussed earlier.[30] A slight enhancement of the heat of fusion with the addition of MWNTs was observed. The heat of fusion is proportional to the amount of crystallinity in the sample, which was also supported by the crystallization behavior of composites. The crytallinity percentage of the LPU was higher than that of the HBPU. This is due to the presence of a large number of branches in the hyperbranched structures, which are responsible for less crystallization.[31]

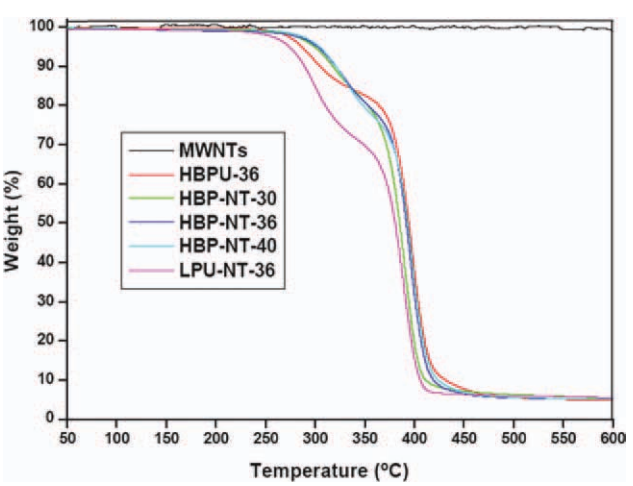

Figure 4. TGA thermograms of pure HBPU, MWNT, and HBPU-MWNT composites. [Color figure can be viewed in the online issue, which is available at wileyonlinelibrary.com.]

Table II. Thermal Properties of Pure HBPU and Its Composites Used in This Study

Sample codes	T_c (°C)	ΔH_c (J/g)	T_m (°C)	ΔH_f (J/g)	Crystallinity (%)
HBPU-36	15.3	61.4	49.3	61.2	31.2
LPU-NT-36	19.5	64.4	49.5	64.1	32.7
HPU-NT-30	18.6	64.6	51.2	63.7	32.8
HPU-NT-36	18.2	63.7	49.9	62.6	32.3
HPU-NT-40	17.5	62.3	47.6	60.3	31.6

Figure 6 presents the stress–strain curves for all the samples. From Figure 6, the breaking stress increased with increasing hard segment content. LPU-NT showed the highest elongation-at-break value. Generally, HBPU has the relatively low mechanical properties because of the fewer chain entanglements and lower viscosity.[32] Owing to their nano-reinforcing effect, the presence of CNTs reinforced the strength and modulus of the HBPU composites with a small decrease in elongation-at-break. In particular, the presence of carboxylic groups of the acid-treated MWNTs is useful for improving the mechanical properties due to the increased hydrogen bonding among the urethane and ester groups of HBPU as discussed earlier (Figure 3).

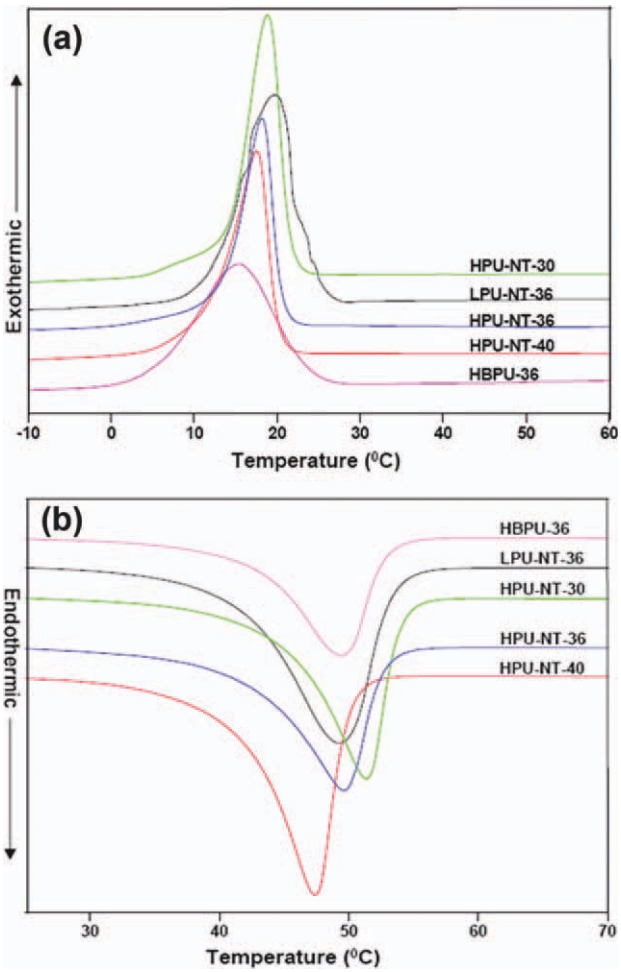

Figure 5. DSC thermograms of pure HBPU and its composites measured during cooling (a) and heating (b). [Color figure can be viewed in the online issue, which is available at wileyonlinelibrary.com.]

The effect of water absorption on the shape memory properties of HBPU and its composites was studied (Figure 7).[33,34] The HBPU and composite films were bent into S shape at 60°C and the deformed shape was retained on quenching into 0°C. The deformed shape could be well kept at room temperature for 1 week with little or no recovery. On the other hand, it recovered its original shape within a few seconds when immersed into water at room temperature. Figure 7 shows the effect of MWNTs addition on the water-responsive shape recovery. The reduced water-responsive shape recovery with MWNTs addition was attributed to the higher crystallization of HBPU by the nanotubes, which makes water diffusion into the HBPU matrix more difficult.[35] The water-absorbed polymers induce the melting of PEG crystals, which become an amorphous PEG component with higher flexibility at ambient temperature.[36] Figure 7 shows the effect of temperature on the shape recovery properties. Faster recovery was observed as the water temperature increased. The shape recovery was just 10 s at 60°C above the melting temperature of the PEG crystals. The rapid recovery is due to the synergistic effect of the thermomechanical and water-responsive shape recovery. The effect of the hard segment content on the water-responsive behavior was also examined. As water absorption depends upon the presence of a hydrophilic PEG content in the segmented PU, the shape recovery was reduced with increasing hard segment content due to decreased PEG content (Figure 8).

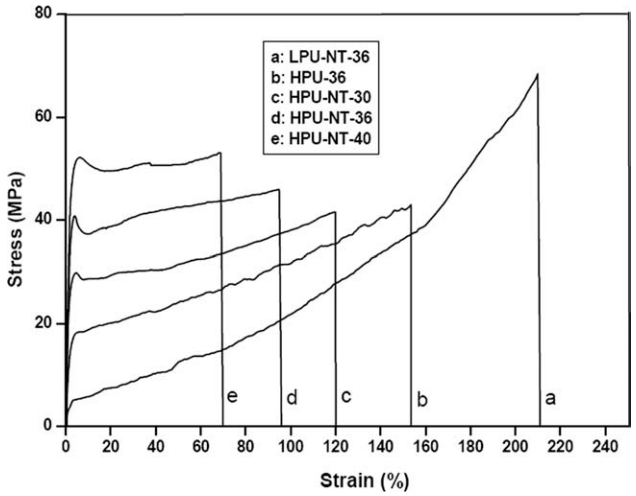

Figure 6. Stress–strain curves of pure HBPU and its composites with different hard segment content.

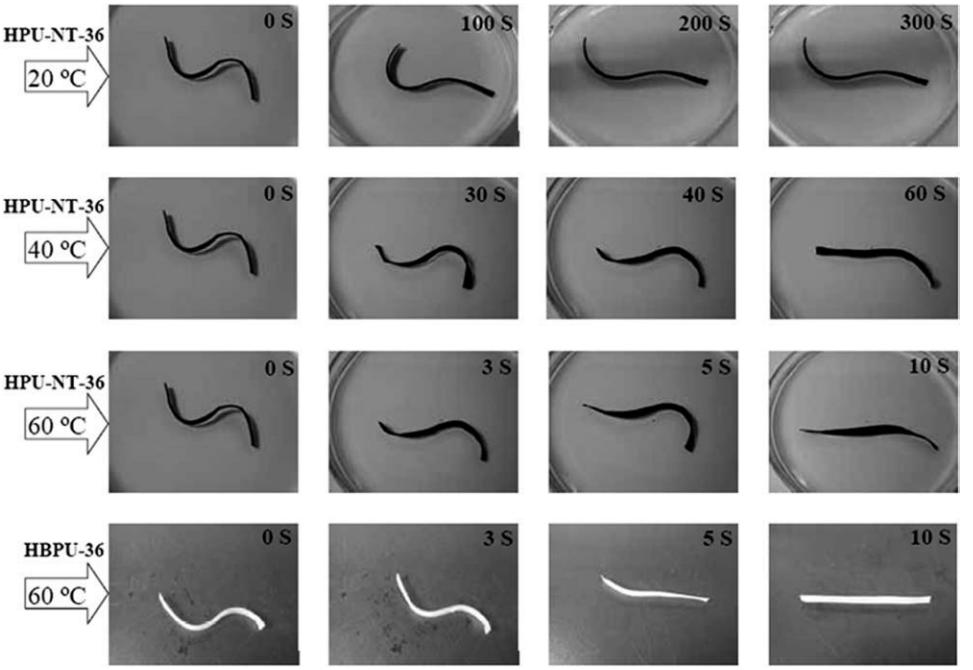

Figure 7. Water-responsive shape recovery behavior of HBPU and its composites at different temperature.

The thermo-mechanical cyclic tensile test was measured when the maximum strain was set to 100% as shown in Figure 9. All the samples showed > 80% shape retention and shape recovery. Table III and Figure 9 show that the shape recovery and shape retention increased with increasing hard segment content of HBPU due to larger number of intermolecular and intramolecular interactions.[5] Their shape memory values were higher for the HBPU composites than the LPU composites, which might be due to the good dispersion of MWNTs in the HBPU matrix, which is useful for obtaining higher recovery owing to the release of stored elastic strain energy.[37] The release of stored elastic strain energy in nanomaterials has been useful for the rapid and more powerful deployment of the composites.[38] The presence of CNTs is also useful for increasing the polymer crystallinity. In particular, the acid functionality of the CNTs tends to make a stronger interaction with the soft segment of the polymer and can increase the crystallinity compared to pristine CNTs.[39]

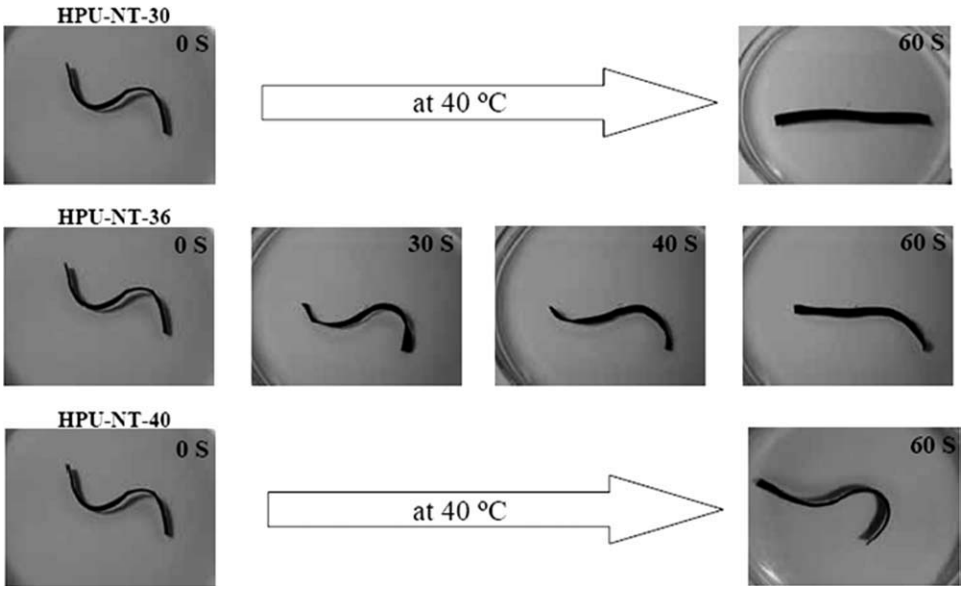

Figure 8. Water-responsive shape recovery behavior of the HBPU-MWNT composites with different hard segment content.

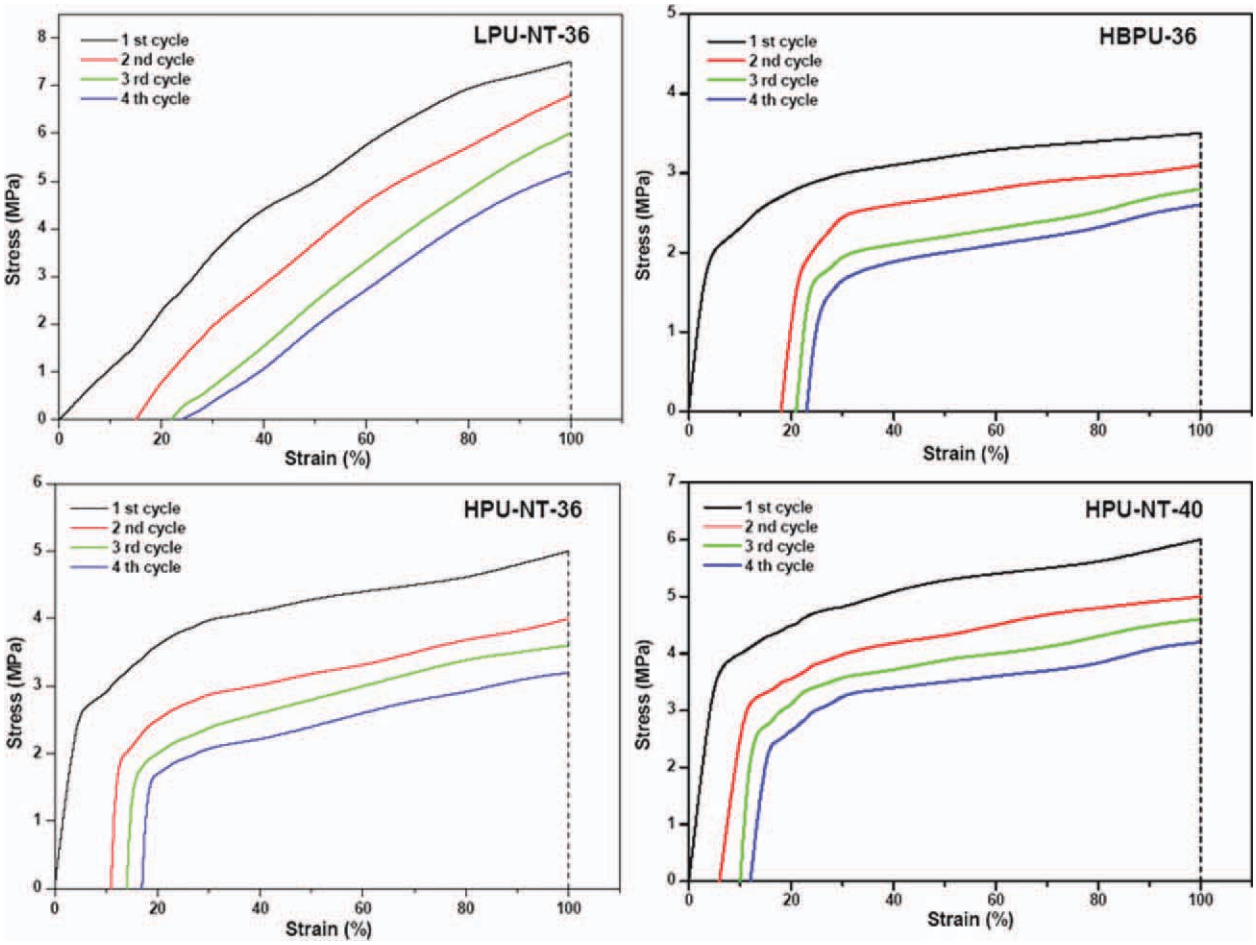

Figure 9. Thermo-mechanical cyclic shape memory tests of the composites. [Color figure can be viewed in the online issue, which is available at wileyonlinelibrary.com.]

The shape recovery force was measured using the equipment set-up in our laboratory[40] (Figure 10). First, the samples were elongated at 100% at 60°C and quenched further to 20°C below the transition temperature of soft segments. The shape recovery force was recorded using a load cell in the tensile force measurement under a constant temperature at 50°C. The shape recovery force increased with increasing hard segment content as well as the presence of MWNTs in the polymer matrix. The hyperbranched polymer composites had a higher shape recovery force than the linear PU composites, which might be due to the stronger molecular interactions of MWNT-COOH with HBPU than linear PU.

CONCLUSIONS

Thermomechanical and water-responsive shape memory hyperbranched PU composites were examined by SEM, TEM, and FTIR. Compared to pure HBPU, the HBPU/MWNT composites showed faster shape recovery and double the shape recovery stress in thermomechanical shape memory test, which was found to be dependent on the MWNTs content and HBPUs hard segments content. The shape recovery stress increased with increasing hard segment content as well as the presence of MWNTs in the polymer matrix. The water-responsive properties decreased with increasing hard segment content due to the lower PEG content. The faster shape recovery of the HBPU

Table III. Values of Shape Retention and Shape Recovery for Pure HBPU and Its Composites After Different Cycles

	Shape retention (%)			Shape recovery (%)		
Sample codes	1st cycle	2nd cycle	3rd cycle	1st cycle	2nd cycle	3rd cycle
HBPU-36	80	75	72	82	79	77
LPU-NT-36	81	78	76	85	80	76
HPU-NT-30	83	77	75	87	82	78
HPU-NT-36	85	79	74	89	86	83
HPU-NT-40	92	87	83	94	90	88

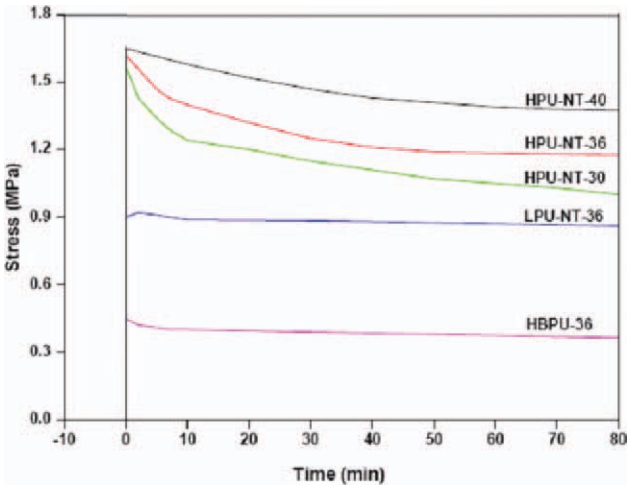

Figure 10. Shape recovery force of HBPU and composites at 50°C. [Color figure can be viewed in the online issue, which is available at wileyonlinelibrary.com.]

composites in water at high temperature was attributed to the synergistic effect of temperature and water absorption.

ACKNOWLEDGMENTS

Contract grant sponsor: Basic Science Research Program through the National Research Foundation of Korea (NRF) funded by the Ministry of Education, Science and Technology; contract grant number: R11-2005-065.

REFERENCES

1. Behl, M.; Lendlein, A. *Mater. Today* **2007,** *10*, 20.
2. Lendlein, A.; Kelch, S. *Angew. Chem. Int. Ed.* **2002,** *41*, 2034.
3. Feninat, F. E.; Laroche, G.; Fiset, M.; Mantovani, D. *Adv. Eng. Mater.* **2002,** *4*, 91.
4. Lendlein, A.; Langer, R. *Science* **2002,** *296*, 1673.
5. Lee, B. S.; Chun, B. C.; Chan, C. Y.; Sul, K. I.; Cho, J. W. *Macromolecules* **2001,** *34*, 6431.
6. Wang, M.; Luo, X.; Ma, D. *Eur. Polym. J.* **1998,** *34*, 1.
7. Yang, J. H.; Chun, B. C.; Chung, Y. C.; Cho, J. W. *Polymer* **2003,** *44*, 3251.
8. Tobushi, H.; Hara, H.; Yamada, E.; Hayashi, S. *Smart Mater. Struct.* **1996,** *5*, 483/1.
9. Wang, Z.; Pinnavaia, T. J. *Chem. Mater.* **1998,** *10*, 3769.
10. Cho, J. W.; Kim, J. W.; Jung, Y. C.; Goo, N. S. *Macromol. Rapid Commun.* **2005,** *26*, 412.
11. Ajayan, P. M.; Stephan, O.; Colliex, C.; Trauth, D. *Science* **1994,** *265*, 1212.
12. Sahoo, N. G.; Rana, S.; Cho, J. W.; Li, L.; Chan, S. H. *Prog. Polym. Sci.* **2010,** *35*, 837.
13. Koerner, H.; Price, G.; Pearce, N. A.; Alexander, M.; Vaia, R. A. *Nat. Mater.* **2004,** *3*, 115.
14. Wei, C.; Srivastava, D.; Cho, K. *Nano Lett.* **2002,** *2*, 647.
15. Liao, K.; Li, S. *Appl. Phys. Lett.* **2001,** *79*, 4225.
16. Rana, S.; Cho, J. W. *Nanoscale* **2010,** *2*, 2550.
17. Andrews, R.; Jacques, D.; Minot, M.; Randell, T. *Macromol. Mater. Eng.* **2002,** *287*, 395.
18. Qin, S.; Qin, D.; Ford, W. T.; Resasco, D. E.; Herrera, J. E. *J. Am. Chem. Soc.* **2004,** *126*, 170.
19. Rana, S.; Karak, N.; Cho, J. W.; Kim, Y. H. *Nanotechnology* **2008,** *19*, 495707/1.
20. Ogoshi, T.; Saito, T.; Yamagishi, T.; Nakamoto, Y. *Carbon* **2009,** *47*, 117.
21. Huang, F.; Gibson, H. W. *J. Am. Chem. Soc.* **2004,** *126*, 14738.
22. Jikei, M.; Kakimoto, M. A. *Prog. Polym. Sci.* **2001,** *26*, 1233.
23. Ogunniyi, D. S. *Bioresorce Technol.* **2006,** *97*, 1086.
24. Karak, N.; Rana, S.; Cho, J. W. *J. Appl. Polym. Sci.* **2009,** *112*, 736.
25. Wunderlich, B. Macromolecular Physics; Academic Press: New York, **1980;** Vol. *3*.
26. Chun, B. C.; Cha, S. H.; Chung, Y. C.; Cho, J. W. *J. Appl. Polym. Sci.* **2002,** *83*, 27.
27. Hawker, C. J.; Lee, R.; Frechet, J. M. J. *J. Am. Chem. Soc.* **1991,** *113*, 4583.
28. Ogoshi, T.; Yamagishi, T.; Nakamoto, Y. *Chem. Commun.* **2007,** *45*, 4776.
29. Chuang, F. S.; Tsen, W. C.; Shu, Y. C. *Polym. Degrad. Stab.* **2004,** *84*, 69.
30. Sahoo, N. G.; Jung, Y. C.; Yoo, H. J.; Cho, J. W. *Macromol. Chem. Phys.* **2006,** *207*, 1773.
31. Magnusson, H.; Malmström, E.; Hult, A.; Johansson, M. *Polymer* **2002,** *43*, 301.
32. Hult, A.; Johansson, M.; Malmstrom, E. *Adv. Polym. Sci.* **1999,** *143*, 1.
33. Huang, W. M.; Yang, B.; An, L.; Li, C.; Chan, Y. S. *Appl. Phys. Lett.* **2005,** *86*, 114105.
34. Yang, B.; Huang, W. M.; Li, C.; Li, L. *Polymer* **2006,** *47*, 1348.
35. Meng, H.; Sui, G. X.; Xie, G. Y.; Yang, R. *Compos. Sci. Technol.* **2009,** *69*, 606.
36. Leng, J.; Lv, H.; Liu, Y.; Du, S. *Appl. Phys. Lett.* **2008,** *92*, 206105/1.
37. Ni, Q. Q.; Zhang, C. S.; Fu, Y.; Dai, G.; Kimura, T. *Compos. Struct.* **2007,** *81*, 176.
38. Goh, H. W.; Goh, S. H.; Xu, G. Q.; Pramoda, K. P.; Zhang, W. D. *Chem. Phys. Lett.* **2003,** *373*, 277.
39. Gunes, S.; Jimenez, G. A.; Jana, S. C. *Carbon* **2009,** *47*, 981.
40. Jung, Y. C.; Cho, J. W. *J. Mater. Sci. Mater. Med.* **2010,** *21*, 2881.